CHEMISTRY OF MATERIALS

Article

pubs.acs.org/cm

Polysulfide-containing Glyme-based Electrolytes for Lithium Sulfur Battery

Marco Agostini,[†] Shizhao Xiong,[‡,§] Aleksandar Matic,[‡] and Jusef Hassoun*[,†]

[†]Department of Chemistry, University of Rome Sapienza, 00185, Rome, Italy

[‡]Department of Applied Physics, Chalmers University of Technology, S41296 Göteborg, Sweden

[§]Department of Materials Science and Engineering, College of Aerospace Science and Engineering, National University of Defense Technology, Changsha, Hunan 410073, PR China

Supporting Information

ABSTRACT: A new comparative investigation of lithium sulfur cells employing a tetraethylene glycol dimethyl ether–lithium trifluoromethanesulfonate (TEGDME-$LiCF_3SO_3$) electrolyte charged by various polysulfide species (Li_2S_2, Li_2S_4, Li_2S_6, and Li_2S_8) is here reported. We carefully detect the effects of lithium polysulfide addition by originally combining X-ray photoelectron spectroscopy (XPS) and electrochemical impedance spectroscopy (EIS). The measurements clearly reveal how the polysulfide addition affects the nature and composition of the solid electrolyte interphase (SEI) in terms of precipitated S-based species determined by XPS. The study demonstrates that the SEI layer formed on the Li anode decreases in impedance and stabilizes by the presence of polysulfide. This, together with a buffer effect strongly mitigating the sulfur-cathode dissolution and the shuttle reaction, significantly improves the stability of the lithium–sulfur cell. The data here reported clearly suggest the polysulfide as an effective additive to enhance the performance of the lithium–sulfur battery.

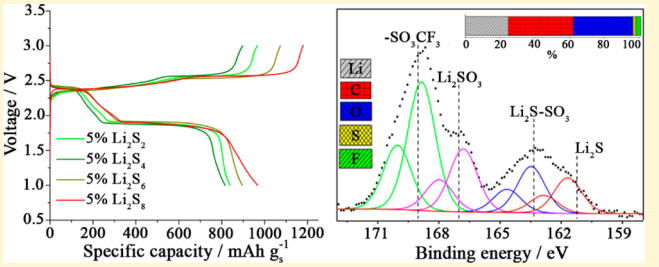

INTRODUCTION

The massive employment of non-renewable fossil fuels has resulted in a rapid increase of greenhouse gas emission and global warming. The consequent excessive climate changes have triggered a new energy policy, mainly focused on clean and renewable sources.[1] Solar and wind energy conversion systems are the most suitable for large-scale diffusion, in particular in view of recent advances reflecting in cost reduction and economic advantages.[1−4] However, these discontinuous energy sources require side systems for energy storage and electrical grid stabilization.[5−7] Furthermore, electrified vehicles using high-energy storage systems matching the automotive market requirements may effectively mitigate the environmental pollution in large urban areas.[2,3] Thus, there is a large push for the development of high capacity energy storage technologies.

The lithium-ion battery (LIB), based on intercalation chemistry, has received considerable attention due to its high energy density, i.e. 450 Wh kg^{-1}, and cycle life.[8] LIBs have had notable success, with mass commercialization, in modern electronic devices. Despite this success, alternative chemistries characterized by higher energy content are required in order to meet the severe targets of the new markets, in particular hybrid and full electric vehicles field. Among the various alternative energy storage systems, the lithium–sulfur battery appears as one of the most promising due to its high theoretical capacity and energy density, i.e. 1672 mAh g^{-1} and 3500 Wh kg^{-1}, respectively, the natural abundance, the low toxicity of elemental sulfur, and the expected low cost.[8−11] However, a sulfur electrode in a lithium battery shows several drawbacks, including poor electronic conductivity, high solubility of the polysulfides formed during the electrochemical process, large volume changes (approximately 80%) by operation, and precipitation of insoluble Li–S intermediates formed during the discharge process in the electrolyte solution. These remarkable issues, leading to severe capacity fading and Li–S cell deterioration upon cycling,[12−14] have been already investigated in terms of the reaction mechanism and the solid electrolyte interphase (SEI) nature, using a bare ether-based electrolyte.[14,15]

Among the various strategies proposed to solve the drawbacks affecting the Li–S battery, the addition of soluble polysulfide species in the electrolyte appeared to effectively enhance the cell performance by mitigating the electrode dissolution.[17−25] Recent papers have demonstrated improvements of the cell characteristics by the addition of polysulfides in solid[16] and liquid electrolytes.[17−25] Indeed, the use of Li_2S_5,[21] Li_2S_6,[17,22] Li_2S_8,[16,19,20,23] and Li_2S_9[18] has shown great influence both on the electrochemical performances[17−20] and on the SEI characteristics and composition.[21−25] The SEI film in lithium sulfur cells plays a crucial role in determining the stability by hindering excessive electrolyte decomposition and

Received: March 9, 2015
Revised: June 10, 2015

DOI: 10.1021/acs.chemmater.5b00896
Chem. Mater. XXXX, XXX, XXX−XXX

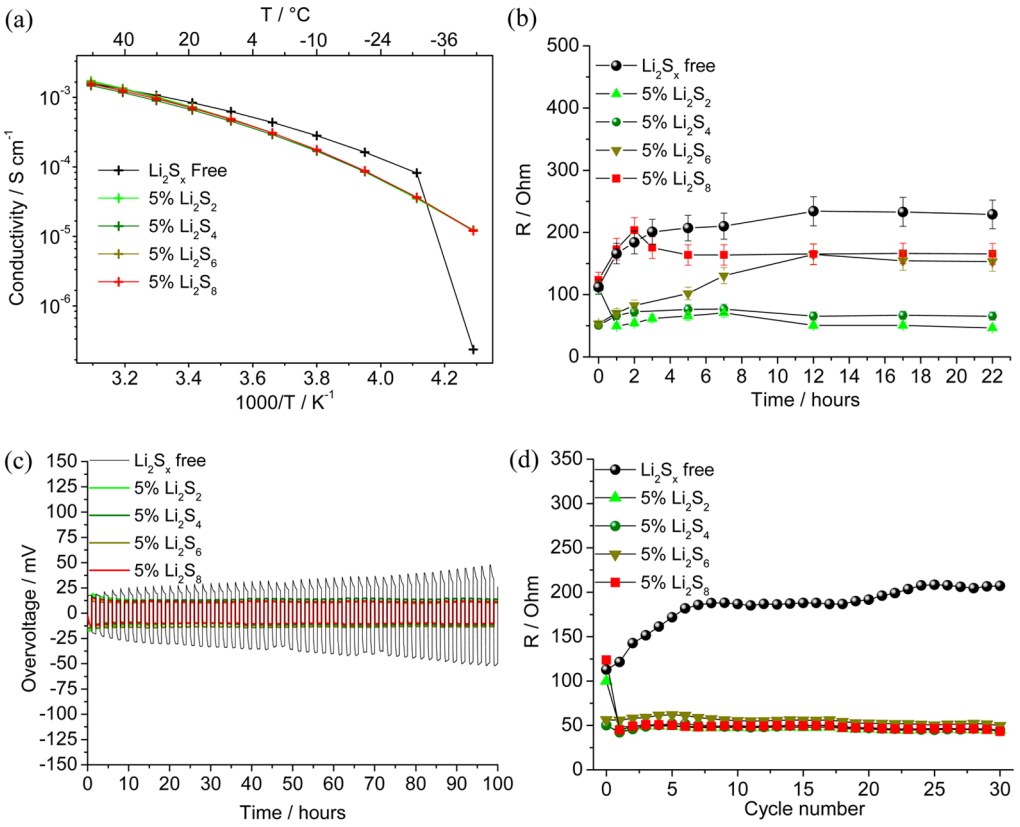

Figure 1. Electrochemical characteristics of the TEGDME-$LiCF_3SO_3$-5%w/w Li_2S_x electrolytes: (a) temperature dependence of the ionic conductivity (Arrhenius plot); (b) time evolution of the resistance in lithium symmetric cells; (c) lithium stripping/deposition overvoltage in lithium symmetric cells cycled at a current of 0.1 mA cm^{-2}; (c) time evolution of the resistance of lithium symmetric cells during the stripping/deposition measurements.

polysulfide-shuttle reaction. However, only a limited amount of papers fully described how the polysulfide behaves at the electrode interphase.

Herein, we reported a detailed study on this important aspect, i.e., the chemical−physical and electrochemical characterization of the electrode−electrolyte interphase. Indeed, we comparatively investigate the properties of the SEI film formed at the lithium electrode surface in tetraethylene glycol dimethyl ether (TEGDME)-based electrolytes containing different polysulfide species, namely Li_2S_2, Li_2S_4, Li_2S_6, and Li_2S_8, added within a constant concentration of 5% w/w, i.e., a value suitable to allow limited viscosity and complete dissolution of the low-soluble polysulfide (e.g., Li_2S_2).[26] The dissolved polysulfide, formally indicated by the stoichiometry Li_2S_x in order to simplify the discussion, is present as a statistic distribution of S chains of various lengths due to disproportionation reaction.[27,28] The various polysulfide species, prepared by changing only the ratio of S to Li and fixing the weight percent of Li_2S_x, have different reactivity with the lithium metal anode in view of the different redox state of sulfur in Li_2S_2, Li_2S_4, Li_2S_6, and Li_2S_8. Accordingly, X-ray photoelectron spectroscopy (XPS) demonstrates that the addition of the polysulfide species to the electrolyte leads to a change in the chemical composition of the SEI layer. Moreover, electrochemical impedance spectroscopy (EIS) reveals an improved compatibility of the high capacity lithium anode with the electrolyte by polysulfide addition, while cycling tests in a lithium sulfur cell clearly show that the buffer effect of the polysulfide prevents the sulfur cathode dissolution, thus improving the cycling performances.

Certainly, an additional investigation, in particular using glyme-based electrolyte with increased amount of polysulfide, is required in order to fully understand the Li−S cell electrochemical behavior and to clarify the contribution of the dissolved species to the SEI film characteristics. However, we believe that the study here reported may shed light on important aspects concerning the improved behavior of the lithium sulfur cell using polysulfide added electrolytes.

RESULTS AND DISCUSSION

TEGDME-$LiCF_3SO_3$ electrolyte solutions containing various polysulfide species, with a 5% fixed weight ratio, have been electrochemically investigated in terms of ionic conductivity and compatibility with the lithium anode in view of possible application in a lithium sulfur cell. The fixed weight ratio of 5% was used in order to allow minimal viscosity changes and preserve the ability of the glyme to dissolve the short-chain polysulfide (e.g., Li_2S_2). The weight ratio was selected instead of molarity to simplify the manuscript discussion by reporting only one parameter (i.e., 5% w/w) instead of various molarities. However, it may be noticed that a 5% w/w solution of a short-chain polysulfide (e.g., Li_2S_4) contains a higher concentration of Li and lower concentration of S compared to a 5% w/w solution of longer chain polysulfide (e.g., Li_2S_8). Furthermore, various polysulfide species of fixed weight % are expected to have different reactivity due to a different redox state of sulfur. Figure 1 shows the conductivity of the electrolyte solutions obtained by using impedance spectroscopy. All investigated electrolytes show a conductivity of about 10^{-3} S cm^{-1} at

DOI: 10.1021/acs.chemmater.5b00896
Chem. Mater. XXXX, XXX, XXX−XXX

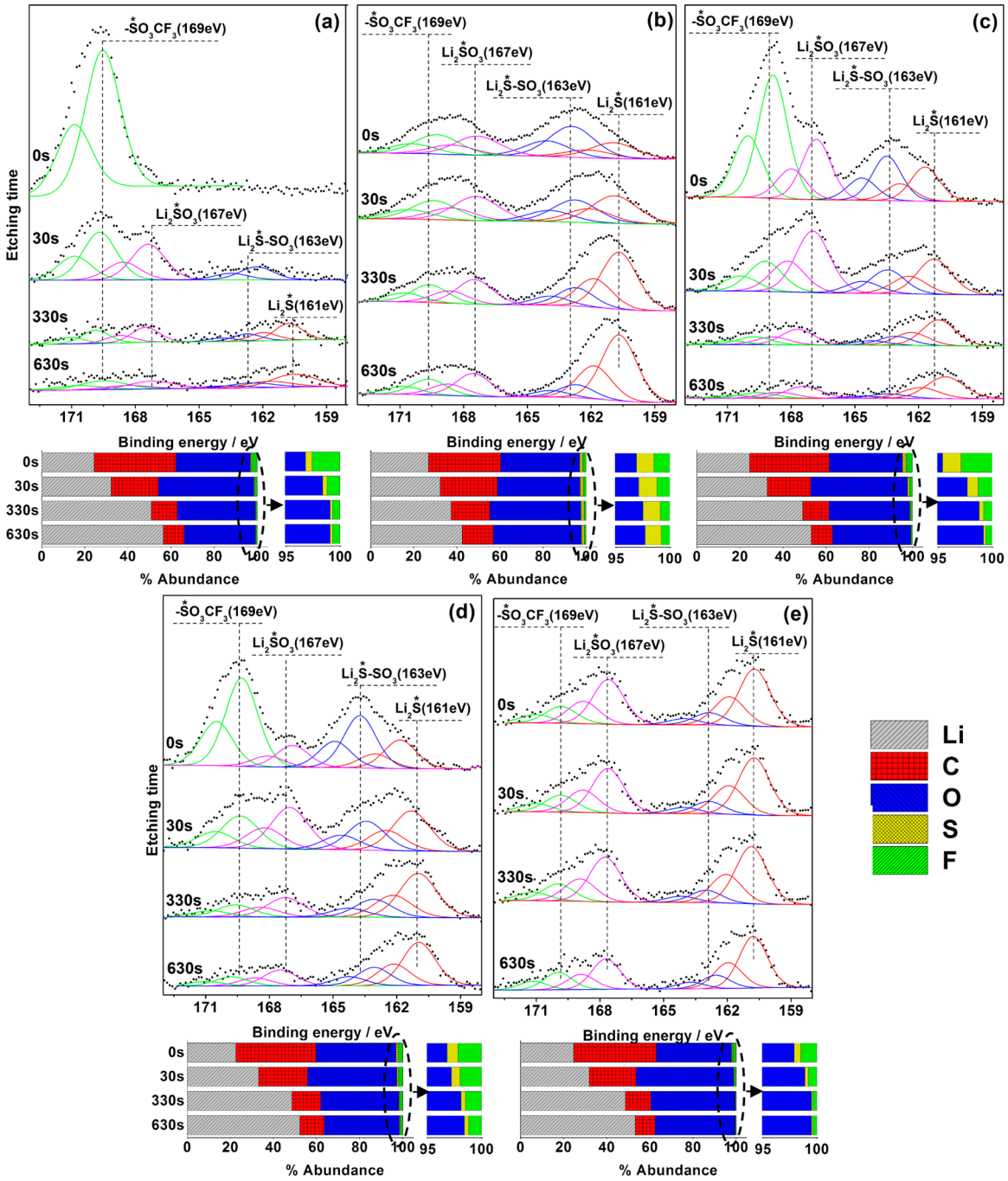

Figure 2. XPS (S 2p) spectra of Li foils soaked into the TEGDME-$LiCF_3SO_3$-5%w/w Li_2S_x electrolytes for 20 days: (a) polysulfide-free electrolyte; (b–e) electrolyte added by Li_2S_2, Li_2S_4, Li_2S_6, and Li_2S_8, respectively. The bottom part of the XPS graphs reports the depth profile (0 s to 630 s) and the % element abundance.

temperatures in the range of 20 to 50 °C, with a very small effect of the polysulfide addition. At lower temperatures, the presence of polysulfides leads to a decrease in the conductivity that remains still around 10^{-4} S cm^{-1} at −25 °C. However, a beneficial effect of the polysulfideaddition is represented by the inhibition of electrolyte crystallization reflecting in a conductivity of about 10^{-5} S cm^{-1} at a temperature as low as −40 °C. In contrast, the neat TEGDME electrolyte is a solid at −40 °C with a very low conductivity, approaching 10^{-7} S cm^{-1}. We expect that the conductivity may slightly change by increasing polysulfide concentration to reach a limit value, determined both by a progressive viscosity rise and by possible ion association due to an increased ionic force of the solution. Further investigation of the electrolyte, in terms of interphase properties with lithium metal, has been performed using electrochemical impedance spectroscopy (EIS). Figure 1b reports the time evolution of the overall resistance (excluding the bulk-electrolyte contribution) of a symmetric lithium cell (see Supporting Information, Figures S1 and S2, for the corresponding Nyquist plots and NLLS fit, respectively). For the neat electrolyte, an initial resistance of about 100 Ω is found with a subsequent increase to about 200 Ω, due to SEI film growth and final stabilization.[19] The polysulfide-containing solutions all show a lower steady state resistance, and a final

DOI: 10.1021/acs.chemmater.5b00896
Chem. Mater. XXXX, XXX, XXX−XXX

value depending on the polysulfide nature (determined by the Li/S ratio). The electrolytes where Li_2S_8 and Li_2S_6 have been added exhibit a stable resistance of about 150Ω, while those based on the shorter polysulfides, Li_2S_2 and Li_2S_4, show a final value limited to about 50 Ω. The electrolyte has also been evaluated with respect to the compatibility with the lithium metal by stripping/deposition galvanostatic measurements, Figure 1c. The neat TEGDME-$LiCF_3SO_3$ solution shows an initial 10 mV stripping/deposition overpotential which increases during cycling to about 50 mV. In contrast, the polysulfide-containing solutions show a stable behavior and a polarization of about 10 mV. The stripping/deposition reaction evolves at around 0 V; that is a value far from the one corresponding to the polysulfide oxidation, generally occurring above 2 V vs Li^+/Li, thus avoiding the polysulfide shuttle reaction. The limited stripping/deposition polarization of the cell using the polysulfide-added electrolytes can be directly related to the lower stable resistance value, as also confirmed by Figure 1d where the resistance evolution during cycling in the lithium symmetrical cell is shown.

The nature and composition of the SEI film at the lithium electrode has been investigated by X-ray photoelectron spectroscopy (XPS). To build up the SEI layer, lithium metal foils were soaked for 20 days in the different electrolyte solutions. Figure 2 reports the XPS spectra, with depth profiling, in the S 2p region, and the %-element abundance determined from the spectra. Generally, the data show the presence of carbon (red), oxygen (blue), and flourine (green) at the lithium surface that can be associated to the break down of the organic components of the electrolyte solution as well as the fluorinated lithium salt. The sulfur (represented by yellow in Figure 2) detected in lithium foils soaked in the polysulfide-free electrolyte is mainly due to the $LiCF_3SO_3$ salt. Furthermore, the lithium foil collected from polysulfide-containing electrolytes shows additional sulfur deposition due to Li_2S_x species. The XPS S 2p spectrum collected from the lithium foil soaked in the neat electrolyte (Figure 2a) shows a pronounced peak at 169 eV (green line) in the top layer, characteristic of the C−SO_3 bonds formed by the partial degradation of the $LiCF_3SO_3$.[15,24,29] With increasing depth, the appearance of three other peaks in the S 2p spectrum can be associated to the formation of Li_2SO_3 (167 eV), Li_2S-SO_3 (163 eV), and Li_2S (161 eV), respectively, due to further degradation of the lithium salt with the formation of kinetically stable products at the solid electrolyte interphase (SEI) film.[15,29] The elemental abundance analysis reveals constant decrease of the C, F, and S concentrations from the surface, thus indicating the formation of the SEI film mainly at the near-metal surface.

The XPS spectra collected from the lithium foils soaked in electrolytes containing polysulfide (Li_2S_x; Figure 2b−e) show the same peaks as the bare solution (i.e., 169 eV, 167 eV, 163 eV, 161 eV), however now observed already on the top surface and with different relative intensities, pointing toward a different SEI formation mechanism. There are also differences between the spectra related to the different electrolyte solutions. The spectra collected from lithium foils soaked in Li_2S_2 and Li_2S_4-containing solutions (Figure 2 b and c, respectively) show a higher sulfur abundance at the surface, 2 ± 0.1%, while the corresponding value for the spectra related to solutions containing Li_2S_6 and Li_2S_8 is lower than 1 ± 0.1%. These data are in line with the resistance trends observed in Figure 1b, suggesting a dependence of the SEI film characteristics on the polysulfide chain length. We may suppose that the lower content of S at the lithium surface in solutions containing the longer chain polysulfide species is due to their higher solubility in the TEGDME solvent.

Galvanostatic charge−discharge tests have been performed using the various electrolyte solutions in lithium/sulfur cells cycled at a C/2 rate. The performance of these cells is reported in Figure 3 in terms of cycling behavior (a), voltage profile (b),

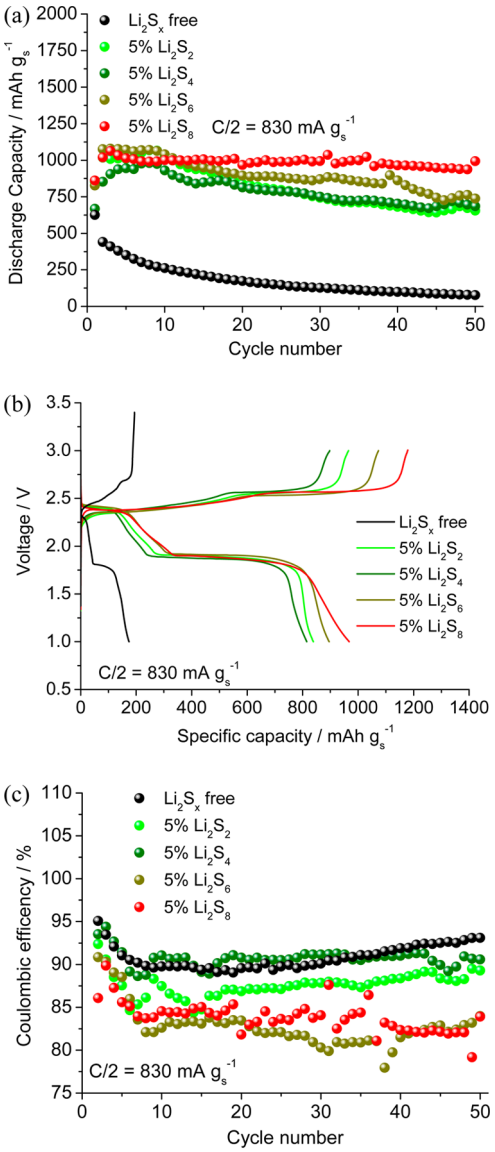

Figure 3. Discharge capacity vs cycle number (a), voltage profiles at the 20th cycle (b), and Coulombic efficiency trends (c) of lithium−sulfur cells galvanostatically cycled at C/2 rate (838 mA g^{-1} referred to the sulfur mass in the cathode) using the various electrolytes. Voltage limits: 1−3.2 V. Room temperature (25 °C).

and Coulombic efficiency (c). The results reveal a very poor behavior for the cell using the neat TEGDME-$LiCF_3SO_3$ electrolyte, characterized by continuous capacity fading upon cycling.[19] A significant improvement is observed when adding the polysulfides to the electrolyte. As seen in Figure 3a, the capacity retention is remarkably enhanced, and the best performance is observed when long chain-length polysulfides are added. In particular, the cell using the Li_2S_8-containing electrolyte delivers a capacity of about 1000 mAh g^{-1} with

DOI: 10.1021/acs.chemmater.5b00896
Chem. Mater. XXXX, XXX, XXX−XXX

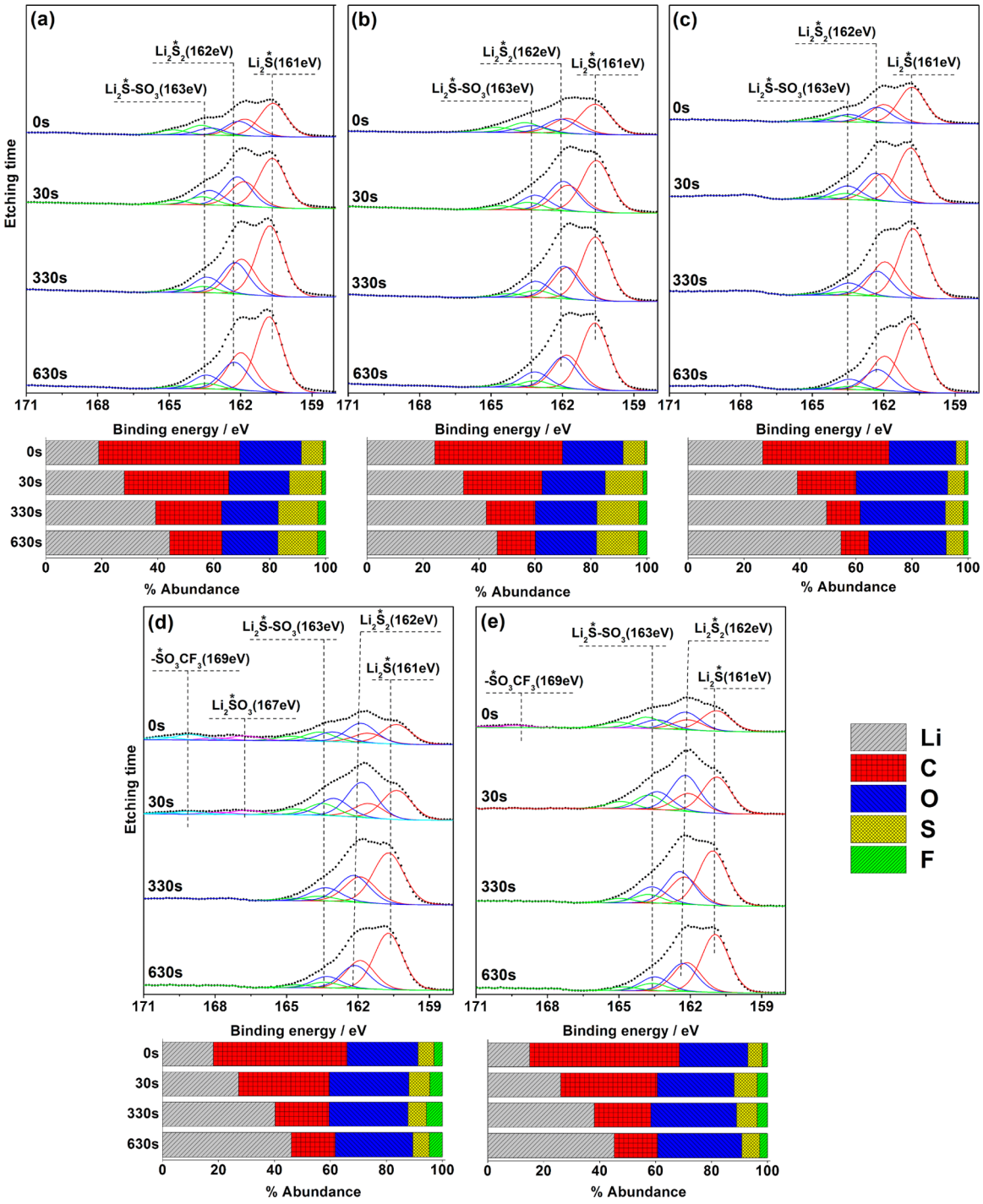

Figure 4. XPS (S 2p) spectra of Li anode recovered after 50 discharge−charge galvanostatic cycles of lithium sulfur cells using TEGDME-$LiCF_3SO_3$ polysulfide-free (a), Li_2S_2-added (b), Li_2S_4-added (c), Li_2S_6-added (d), Li_2S_8-added (e) electrolyte solution. The bottom part of the XPS graphs reports the depth profile (0s to 630s) and the % element abundance.

respect to the sulfur loaded in the catode after 50 cycles, i.e., a value considered suitable for ensuring the full formation of the SEI layer at the electrodes surface, thus allowing a proper evaluation of the interphase characteristics and of the polysulfide role in mitigating the sulfur dissolution and the shuttle reaction. We have also reported in the Supporting Information, Figure S3, the cycling behavior referring to the overall sulfur amount, i.e., including the sulfur in the electrode and in the electrolyte solution. As expected, the overall cell capacity is reduced by about 5 to 15% due to the low contribution of the dissolved polysulfide mass to the overall specific capacity. The direct polysulfide contribution to the electrochemical process in Li/S cell strongly depends on the nature of the carbon used at the cathode side and may be, for example, promoted by using high surface carbons.[23] Indeed, we demonstrated in a previous paper that cells using the configuration here adopted exploit only in small part the dissolved polysulfide as active material. In our case, the polysulfide acts mainly as a mass buffer avoiding the electrode dissolution.[19] Figure 3b shows the voltage profiles at the 20th

DOI: 10.1021/acs.chemmater.5b00896
Chem. Mater. XXXX, XXX, XXX−XXX

cycle which can be considered as steady state. These profiles reveal a high charge−discharge polarization and limited capacity for the cell using the neat electrolyte, whereas the overvoltage is limited to about 0.4 V for the polysulfide-containing solutions. However, the Coulombic efficiency (Figure 3c) as well as the final energy efficiency (Figure S4 in Supporting Information section) appear higher for the cell with the neat electrolyte and a decreasing efficiency is observed when electrolytes with increasing polysulfide chain-length are used. To be noticed that the cell using Li_2S_6 polysulfide shows a different capacity trend, still to be fully clarified, most likely due to a different dissolution kinetic at the cathode side. The results of Figure 3 may be tentatively explained by taking into account the three following phenomena occurring at the electrode−electrolyte interphase in a lithium sulfur cell: (i) cathode dissolution; (ii) polysulfide shuttle reaction; and (iii) insoluble Li_2S_x species precipitation at the lithium side. The capacity fading in the cell with neat electrolyte can be explained by an excessive cathode dissolution, with formation of Li_2S_x and its fast deposition at the lithium surface. In contrast, the presence of the soluble Li_2S_8 polysulfide in the electrolyte, in addition to an improved SEI film (see Figure 2e and related discussion), efficiently buffers the cathode dissolution, accounting for the improved cycle life of the cell. However, the permanent presence of a dissolved polysulfide species in the electrolyte causes partial shuttle reactions which decreases the overall efficiency of the cell reaction. The cells using the electrolytes containing Li_2S_6 and Li_2S_2 show an intermediate behavior with some capacity fading and a lower efficiency, involving partial dissolution and deposition of insoluble species at the lithium surface. The cell using the electrolyte added by Li_2S_4 shows a high efficiency, comparable to the cell with the neat electrolyte and a satisfactory capacity, however characterized by slight decay upon cycling.

The above findings are partially supported by an XPS analysis performed on lithium anodes recovered from the cells after 50 discharge−charge cycles, Figure 4. The spectra show a higher sulfur content, both at the surface and deeper down in the SEI layer, compared to the pristine electrodes just soaked in the electrolyte solutions (compare Figures 2 and 4). In particular, the spectra related to the polysulfide-free and Li_2S_2-containing electrolyte solutions reveal an overall higher sulfur content, suggesting extensive Li_2S_x deposition. Considering the absence of dissolved polysulfides in the pristine state of the neat electrolyte, the large presence of sulfur at the lithium surface after cycling confirms dissolution of the sulfur electrode and the following fast precipitation at the Li-anode side, accounting for the strong capacity fade (see Figure 3a). In the case of the Li_2S_2-containing solution, this points toward a less effective buffer action of the electrolyte, and it is prone to excessive precipitation of the insoluble Li_2S_2 at the Li surface. Instead, the cells using electrolytes containing polysulfide species of intermediate length, i.e. Li_2S_4 and Li_2S_6, seem to have a much better buffering ability manifested in less dissolution of the cathode and thereby less tendency of shuttling of the easily precipitating polysulfide species, i.e. Li_2S_2, formed at the cathode during the end of discharge.

■ CONCLUSION

We have investigated the effect of various polysulfide species addition to a TEGDME-$LiCF_3SO_3$ electrolyte solution used for Li−S batteries. We evaluated both the role of anode interphase and cathode performances demonstrating the effect of the film formed at the Li surface. Indeed, particular attention has been devoted to the study, by XPS and EIS measurements, of the solid electrolyte interphase (SEI) at the lithium electrode. The data suggested that the SEI film composition and nature depend on the added polysulfide species, directly affecting the lithium sulfur cell performance in terms of capacity, efficiency, and cycle life. The room temperature SEI stability upon polysulfide addition, empirically demonstrated by the EIS, has been ascribed to the formation of a protecting layer of precipitated polysulfide species covering the lithium surface, thus kinetically avoiding further reaction with the electrolyte bulk. Indeed, the formation of this protective layer is revealed by the XPS spectra. The stability of the SEI upon polysulfide addition, reported also in previous papers,[16,17,19] is further demonstrated during cycling. The results indicate that solutions containing the longer polysulfides, e.g. Li_2S_8, are the most promising with respect to the formation of a stable SEI layer and an improved buffering action of the polysulfide, thus leading to limited sulfur cathode dissolution and higher cell stability.

■ EXPERIMENTAL SECTION

Polysulfide containing electrolyte solutions were prepared by first dispersing lithium metal (Chemetall) and elemental sulfur (Aldrich) in a molar ratio of 2:2, 2:4, 2:6, and 2:8, respectively, in the TEGDME solvent (Aldrich) with a final Li_2S_x/solvent weight ratio of 5% w/w. The mixtures were heated at 80 °C for 24 h to obtain homogeneous solutions, with no precipitated sulfur or lithium metal residuals. During preparation at 80 °C, the formation of polysulfide by reacting lithium and sulfur required the use of very small pieces of lithium metal, in order to kinetically promote the full conversion to Li_2S_x species. Subsequently, 1 mol/kg $LiCF_3SO_3$ was added to the TEGDME-polysulfide solution. The sulfur−carbon electrode was prepared according to a procedure reported previously,[30] i.e. by melting sulfur at 130 °C and mixing it with MCMB (mesocarbon microbeads) in a weight ratio of 1:1. Stainless steel electrodes (SS, diameter 10 mm) were used in a SS/electrolyte/SS symmetric cell with Teflon O-ring spacers, at a thickness of 1 mm, to measure the ionic conductivity of the electrolytes in the temperature range of −40 to 50 °C. The measurements were carried out on a Novocontrol broadband dielectric spectrometer in the frequency range of 0.01−1 MHz. The lithium-electrolyte interphase resistance was studied by EIS (electrochemical impedance spectroscopy) applying a 10 mV AC amplitude signal to a Li symmetrical cell in a 500 kHz to 100 mHz frequency range. The interphase resistance and the charge transfer resistance were evaluated by nonlinear least-squares (NLLS) fit of the semicircles observed in the Nyquist plots. The Nyquist plots related to the stability of polysulfide-added electrolytes, showing the semicircles associated to film formation and charge-transfer processes, located at high and low frequency regions, respectively, are reported in Figure S1 of the Supporting Information. The equivalent circuit used for the NLLS fit was R(RQ)(RQ)Q, were R represents the resistance and Q the constant phase element (CPE). The error bar related to the resistance evaluation was extrapolated by error distribution study, including instrumental errors, as well as the error associated to the cell reproducibility (i.e., calculated by repeating the measurement in various cells using the same material). This study has led to an error bar of 10%. The lithium stripping/deposition test was performed galvanostatically using a 0.1 mA cm^{-2} current in a Li-symmetrical cell. EIS

DOI: 10.1021/acs.chemmater.5b00896
Chem. Mater. XXXX, XXX, XXX−XXX

measurements after discharge−charge were performed using the same cell during cycling. All the above tests were performed by using 2032 coin-type cells with a 1.6 cm internal diameter (2.01 cm^2 surface) and a VSP Biologic instrument. XPS measurements were performed on lithium foils soaked in the electrolyte solution for 20 days as well as upon 50 charge−discharge cycles. Prior to the experiments, the foils were washed by dimethyl carbonate (DMC) to remove residual electrolyte or precipitated $LiCF_3SO_3$ salt on the surface, thus avoiding possible contributions to the XPS signal, and subsequently dried for 30 min under a vacuum to remove residual DMC solvent. The process was carried out in an Ar glovebox (MBraunLabstar, H_2O <0.1 ppm,O_2 < 0.1 ppm). An argon atmosphere controlled glovebag (Aldrich) was employed to transfer the samples from the glovebox to the chamber of the XPS systems (PHI 5800, Physical Electronics). The sealed glovebag was subsequently connected to the entrance of the chamber of XPS. High-purity argon was used to refill the bag several times, and the sample stage was transferred into the XPS system under argon, without any exposure to air. The X-ray source for the XPS analysis was an Al Kα radiation (200W, 13 kV), the chamber pressure 10^{-9} Torr, and the diameter of the analyzed surface 800 μm. The etching process was performed by an argon ion beam (accelerating voltage 3 kV, emission current 10 mA, etching area, 1 mm × 1 mm). The spectra were calibrated by the binding energy of the C 1s peak (BE = 284.5 eV). All spectra were fitted by the deconvolution software (Casa XPS, Casa Software). A Monte Carlo simulation has been performed for each spectrum in the atomic concentration calculation to obtain the integrating error. Gaussian−Lorentzian (30% Gaussian) functions and a Shirley-type background were employed in all fitting spectra. The peak fitting was limited as follows: the full width at half-maximum of all component peaks was equal; the position between S $2p_{3/2}$ and S $2p_{1/2}$ was fixed to 1.18 eV; the peak area ratio of $S2p_{3/2}$ and S $2p_{1/2}$ was fixed to 2:1. According to the XPS integrating standard errors, the sulfur abundance at the surface of the lithium soaked in Li_2S_2, Li_2S_4, Li_2S_6, and Li_2S_8-containing solutions is 2.000 ± 0.132%, 2.000 ± 0.002%, 1.000 ± 0.058%, and 0.800 ± 0.050%, respectively. The galvanostatic cycling tests were performed in lithium half-cells using a Whatman separator soaked by a low electrolyte volume (of 30 μL as determined by micropipette) at a current of 830 mA g^{-1}, referring to the sulfur mass in the electrode material, within a voltage range of 1−3 V, at 25 °C using a Maccor series instrument. Considering the electrolyte amount in the glass fiber normalized in respect to the electrode surface (16 mm of diameter, 2 cm^2 of surface, and 15 $\mu L/cm^{-2}$ of electrolyte), we can calculate a Li_2S_x polysulfide loading of 0.75 mg cm^{-2}, with a sulfur concentration depending on the chain length of the added polysulfide (i.e., 0.71 mg cm^{-2} for Li_2S_8, 0.533 mg cm^{-2} for Li_2S_6, 0.355 mg cm^{-2} for Li_2S_4, 0.177 mg cm^{-2} for Li_2S_2). The sulfur loading in the electrode (13 mm diameter) was of 2 mg cm^{-2}. Considering these data, Figure S3 in the Supporting Information reports the cycling test of Figure 3a referring the capacity to the overall sulfur loading (electrode and electrolyte).

■ ASSOCIATED CONTENT

Supporting Information

Figures S1−S4 and additional text. The Supporting Information is available free of charge on the ACS Publications website at DOI: 10.1021/acs.chemmater.5b00896.

■ AUTHOR INFORMATION

Corresponding Author

*E-mail: jusef.hassoun@uniroma1.it.

Notes

The authors declare no competing financial interest.

■ REFERENCES

(1) Armand, M.; Tarascon, J.-M. Building better batteries. *Nature* **2008**, *451*, 652−657.

(2) Scrosati, B. Challenge of portable power. *Nature* **1995**, *373*, 557−558.

(3) Yang, Y.; Zheng, G.; Cui, Y. Nanostructured sulfur cathodes. *Chem. Soc. Rev.* **2013**, *42*, 3018−3032.

(4) Tarascon, J.-M.; Armand, M. Issues and challenges facing rechargeable lithium batteries. *Nature* **2001**, *414*, 359−367.

(5) Bruce, P. G.; Freunberger, S. A.; Hardwick, L. J.; Tarascon, J.-M. Li-O_2 and Li-S batteries with high energy storage. *Nat. Mater.* **2012**, *11*, 19−29.

(6) Scrosati, B.; Garche, J. Lithium batteries: Status, prospects and future. *J. Power Sources* **2010**, *195*, 2419−2430.

(7) Whittingham, M. S. Lithium Batteries and Cathode Materials. *Chem. Rev.* **2004**, *104*, 4271−4301.

(8) Manthiram, A. Materials Challenges and Opportunities of Lithium Ion Batteries. *J. Phys.Chem. Lett.* **2011**, *2*, 176−184.

(9) Ji, X.; Nazar, L. F. Advances in Li-S batteries. *J. Mater. Chem.* **2010**, *20*, 9821−9826.

(10) Hassoun, J.; Agostini, M.; Latini, A.; Panero, S.; Sun, Y.-K.; Scrosati, B. Nickel-Layer Protected, Carbon-Coated Sulfur Electrode for Lithium Battery. *J. Electrochem. Soc.* **2012**, *159*, A390−A395.

(11) Hassoun, J.; Scrosati, B. Moving to a Solid-State Configuration: A Valid Approach to Making Lithium-Sulfur Batteries Viable for Practical Applications. *Adv. Mater.* **2010**, *22*, 5198−5201.

(12) Dominko, R.; Demir-Cakan, R.; Morcrette, M.; Tarascon, J.-M. Analytical detection of soluble polysulphides in a modified Swagelok cell. *Electrochem. Commun.* **2011**, *13*, 117−120.

(13) Nelson, J.; Misra, S.; Yang, Y.; Jackson, A.; Liu, Y.; Wang, H.; Dai, H.; Andrews, J. C.; Cui, Y.; Toney, M. F. In Operando X-ray Diffraction and Transmission X-ray Microscopy of Lithium Sulfur Batteries. *J. Am. Chem. Soc.* **2012**, *134*, 6337−6343.

(14) Ryu, H.-S.; Guo, Z.; Ahn, H.-J.; Cho, G.-B.; Liu, H. Investigation of discharge reaction mechanism of lithium liquid electrolyte sulfur battery. *J. Power Sources* **2009**, *189*, 1179−1183.

(15) Ota, H.; Sakata, Y.; Wang, X.; Sasahara, J.; Yasukawa, E. Characterization of Lithium Electrode in Lithium Imides/Ethylene Carbonate and Cyclic Ether Electrolytes II. Surface Chemistry. *J. Electrochem. Soc.* **2004**, *151*, A437−446.

(16) Agostini, M.; Hassoun, J. A lithium-ion sulfur battery using a polymer, polysulfide-added membrane. *Sci. Rep.* **2015**, *5*, 7591.

(17) Chen, S.; Dai, F.; Gordin, M. L.; Wang, D. Exceptional electrochemical performance of rechargeable Li-S batteries with a polysulfide-containing electrolyte. *RSC Adv.* **2013**, *3*, 3540−3543.

(18) Zhang, S. S.; Read, J. A. A new direction for the performance improvement of rechargeable lithium/sulfur batteries. *J. Power Sources* **2012**, *200*, 77−82.

(19) Lee, D.-J.; Agostini, M.; Park, J.-W.; Sun, Y.-K.; Hassoun, J.; Scrosati, B. Progress in Lithium-Sulfur Batteries: The effective Role of a Polysulfide-Added Electrolyte as Buffer to prevent Cathode Dissolution. *ChemSusChem* **2013**, *6*, 2245−2248.

(20) Yang, Y.; Zheng, G.; Cui, Y. A membrane-free lithium/polysulfide semi-liquid battery for large scale energy storage. *Energy Environ. Sci.* **2013**, *6*, 1552−1558.

(21) Demir-Cakan, R.; Morcrette, M.; Gangulibabu; Guéguen, A.; Dedryvère, R.; Tarascon, J.-M. Li-S batteries: simple approaches for superior performance. *Energy Environ. Sci.* **2013**, *6*, 176−182.

(22) Xiong, S.; Xie, K.; Diao, Y.; Hong, X. Characterization of the solid electrolyte interphase on lithium anode for preventing the shuttle mechanism in lithium-sulfur batteries. *J. Power Sources* **2014**, *246*, 840−845.

DOI: 10.1021/acs.chemmater.5b00896
Chem. Mater. XXXX, XXX, XXX−XXX

(23) Agostini, M.; Lee, D.-J.; Scrosati, B.; Sun, Y.-K.; Hassoun, J. Characteristics of Li_2S_8-tetraglyme catholyte in a semi-liquid lithium-sulfur battery. *J. Power Sources* **2014**, *265*, 14−19.
(24) Diao, Y.; Xie, K.; Xiong, S.; Hong, X. Shuttle phenomenon-The irreversible oxidation mechanism of sulfur active material in Li-S battery. *J. Power Sources* **2013**, *235*, 181−186.
(25) Xiong, S.; Xie, K.; Blomberg, E.; Jacobsson, P.; Matic, A. Analysis of the solid electrolyte interphase formed with an ionic liquid electrolyte for lithium-sulfur batteries. *J. Power Sources* **2014**, *252*, 150−155.
(26) Li, Y.; Zhan, H.; Liu, S.; Huang, K.; Yunhong, K. Electrochemical properties of the soluble reduction products in rechargeable Li/S battery. *J. Power Sources* **2010**, *195*, 2945−2949.
(27) Feng, Z.; Kim, C.; Vijh, A.; Armand, M.; Bevan, K. H.; Zaghib, K. Unravelling the role of Li2S2 in lithium-sulfur batteries: A first principles study of its energetic and electronic properties. *J. Power Sources* **2014**, *272*, 518−521.
(28) Park, H.; Koh, H. S.; Siegel, D. J. First Principles Study of Redox End-Members in Lithium-Sulfur Batteries. *J. Phys. Chem. C* **2015**, *119*, 4675−4683.
(29) Foix, D.; Gonbeau, D.; Taillades, G.; Pradel, A.; Ribes, M. The structure of ionically conductive chalcogenide glasses: a combined NMR, XPS and ab initio calculation study. *Solid State Sci.* **2001**, *3*, 235−243.
(30) Agostini, M.; Ahiara, Y.; Yamada, T.; Scrosati, B.; Hassoun, J. A lithium-sulfur battery using a solid, glass-type P_2S_5-Li_2S electrolyte. *Solid State Ionics* **2013**, *244*, 48−51.

DOI: 10.1021/acs.chemmater.5b00896
Chem. Mater. XXXX, XXX, XXX−XXX